Electronic Supplementary Information

Dangling carboxylic-acid functionality in a fish-bone-shaped 2D framework as a hydrogen-bond-donating catalyst in Friedel-Crafts alkylation

Nilanjan Seal[a,b] and Subhadip Neogi*[,a,b]

[a]Academy of Scientific and Innovative Research (AcSIR), Ghaziabad- 201002, India
[b]Inorganic Materials & Catalysis Division, CSIR-Central Salt & Marine Chemicals Research Institute, Bhavnagar, Gujarat 364002, India
**E-mail address*: sneogi@csmcri.res.in (S. Neogi)

Table of contents

Section S1. Materials and Physical measurements

All the solvents and reagents were purchased from commercial sources (except H_3TCA) and used without further purification. Powder X-ray diffraction (PXRD) data were collected using a PANalytical Empyrean (PIXcel 3D detector) system equipped with Cu Kα (λ=1.54 Å) radiation. The Fourier Transform Infrared-spectra (IR) of the samples were recorded using the KBr pellet method on a Perkin–Elmer GX FTIR spectrometer in the region of 4000−400 cm^{-1}. Thermogravimetric analyses (TGA) (heating rate of 5 °C/min under N_2 atmosphere) were performed with a Mettler Toledo Star SW 8.10 system. Surface area measurement was carried out using Quantachrome Autosorb IQ instrument. ^{1}H NMR spectra were recorded on a Bruker

Avance-II 500 MHz NMR spectrometer. Scanning Electron Microscopic (SEM) images were obtained with a JEOL JSM 7100F instrument. Inductively coupled plasma-mass spectrometry (ICP-MS) analysis was measured by Perkin Elmer, Optima 2000. XPS analysis was carried out using a Thermo Scientific ESCALAB 250 Xi photoelectron spectrometer (XPS) using a monochromatic Al Kα X-ray as an excitation source.

Section S2. Single Crystal X-ray Crystallography

Single crystals with suitable dimensions were chosen under an optical microscope and mounted on a glass fibre for data collection. The crystal data for **CSMCRI-21** and **CSMCRI-28** were collected on a Bruker D8 Quest diffractometer, with CMOS detector in shutter less mode. The crystals were cooled to low temperature using an Oxford Cryostream liquid nitrogen cryostat. The instrument was equipped with a graphite monochromatized MoKα X-ray source (λ = 0.71073 Å), with Triumph™ X-ray source optics. Data collection and initial indexing and cell refinement were handled using APEX II software.[1] Frame integration, including Lorentz-polarization corrections, and final cell parameter calculations were carried out using SAINT+ software.[2] The data were corrected for absorption using the SADABS program.[3] Decay of reflection intensity was monitored by analysis of redundant frames. The structure was solved using Direct methods and difference Fourier techniques. All non-hydrogen atoms were refined anisotropically. All H atoms were placed in calculated positions using idealized geometries (riding model) and assigned fixed isotropic displacement parameters. The SHELXL-2014 package within the OLEX2 crystallographic software[4] was applied for structure refinement with several full-matrix least-squares/difference Fourier cycles.[5] The disordered guest solvent molecules in the crystal lattice were treated with solvent mask option in OLEX2 software.[4] The potential solvent accessible void space was calculated using the PLATON[6] software. The crystal and refinement data for **CSMCRI-21** and **CSMCRI-28** are listed in Table S1 and Table S3, respectively. Topological analysis was performed by using ToposPro software.[7]

Section S3. Experimental Section

Synthesis of the Ligand

The ligand, 4,4',4"-tricarboxytriphenylamine (H_3TCA) was prepared and characterized according to literature methods.[8]

Synthesis of CSMCRI-21. A mixture of $Co(NO_3)_2 \cdot 6H_2O$ (11.63 mg, 0.04 mmol), dpa (7.36 mg, 0.04 mmol) and H_3TCA (7.54 mg, 0.02 mmol) was dissolved in 1.5 mL of N,N-Dimethylformamide (DMF) and 1.5 mL of water in a 15 mL screw-capped vial. After that, it was heated to 100 °C for three days, and then slowly cooled down to room temperature. The orange colored, block shaped crystals were obtained; which were then filtered and thoroughly washed with DMF. Anal. Calcd. For $[Co_3(TCA)_3(dpa)_3] \cdot 3DMF \cdot 7H_2O$: C, 55.74; H, 4.36; N, 11.47. Found: C, 55.78; H, 4.39; N, 11.46.

Synthesis of CSMCRI-28. The synthetic procedure for **CSMCRI-28** is similar to that of **CSMCRI-21** except the fact that H_2OBA (5.16 mg, 0.02 mmol) was used instead of H_3TCA. [H_2OBA : 4,4′-Oxybis(benzoic acid)]

General procedure for Friedel-Crafts reaction and calculation of yield (%). Indoles (0.15 mmol), β-nitrostyrenes (0.1 mmol), 3.6 mol % catalyst (**21a**) and 1 mL toluene were taken in a reaction tube (5 mL) and the mixture was stirred at 60 °C for 12 h. After the reaction is completed, it was centrifuged to separate the catalyst followed by removal of solvent under reduced pressure. The crude products were analysed through ^{1}H NMR spectroscopy using 1,3,5-trimethoxybenzene as internal standard. Yields (%) of the products were determined from the integral area of internal standard (9H at 3.77 ppm) and products (4.92-5.25 ppm). After thorough washing of the recovered catalyst with dichloromethane, it was undergone further characterization and recycling study.

Synthesis of Ni^{2+}@21a. 50 mg of activated MOF and 20 mg of $NiCl_2 \cdot 6H_2O$ were taken in 20 mL of methanol. The mixture was stirred at 50 °C for 2 h, followed by filtration and thorough washing with methanol. Finally, the obtained derived material was dried at 60 °C for 4 h to get Ni^{2+}@**21a**, which was further characterized and used in performing reaction.

a)

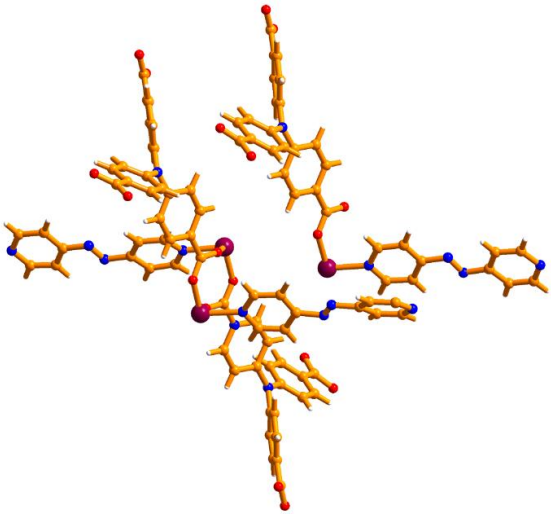

b)

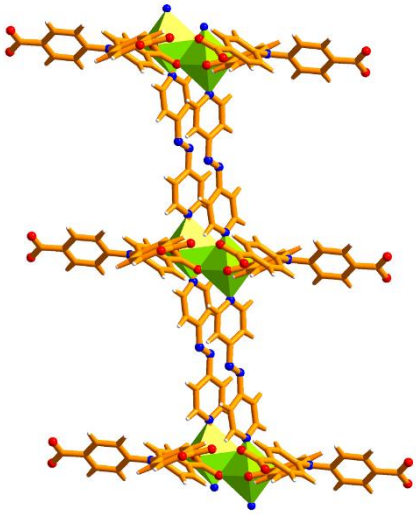

c)

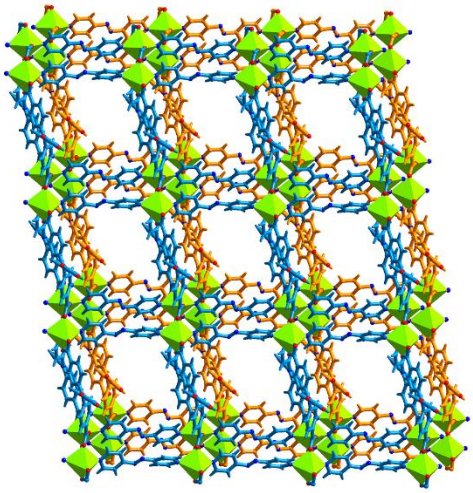

d)

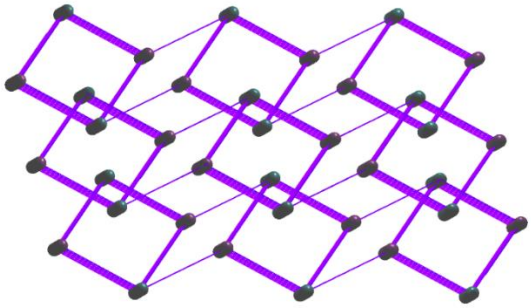

Fig. S1 (a) Asymmetric unit of **CSMCRI-21**. (b) Fish-bone shaped architecture of the MOF. (c) Layer-stacked interdigitated structure of the framework. (d) Topological representation of **CSMCRI-21**.

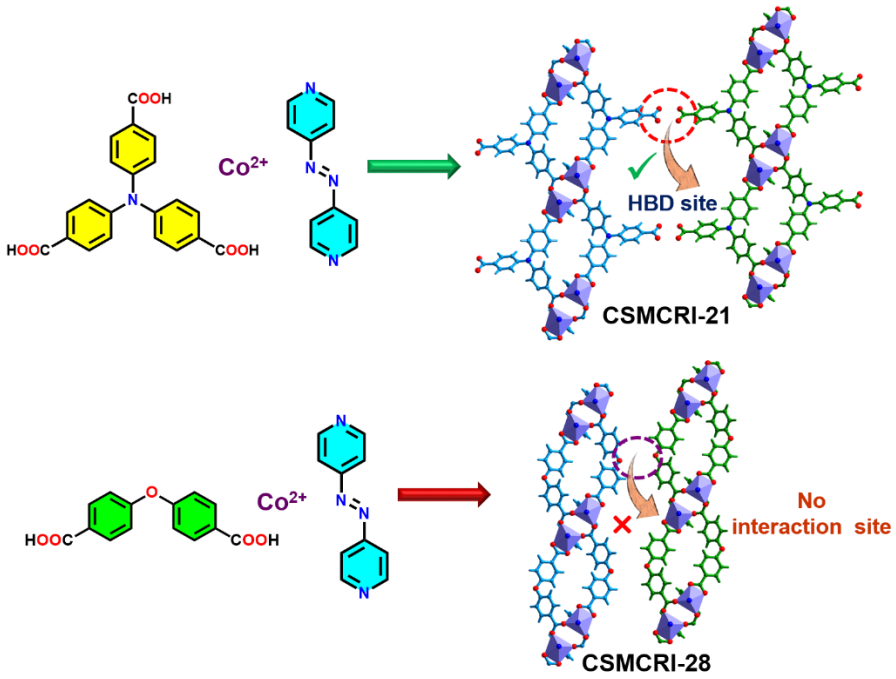

Scheme S1. Schematic representation for the synthesis of **CSMCRI-21** and isostructural **CSMCRI-28** along with presence of hydrogen-bond-donating catalytic site (oppositely faced –COOH moieties) in the former structure.

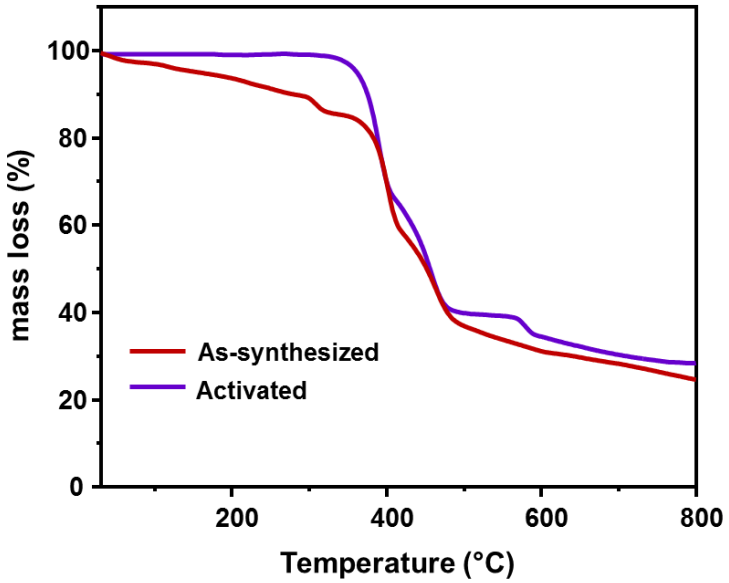

Fig. S2 Thermogravimetric analysis (TGA) of as-synthesized and activated **CSMCRI-21**.

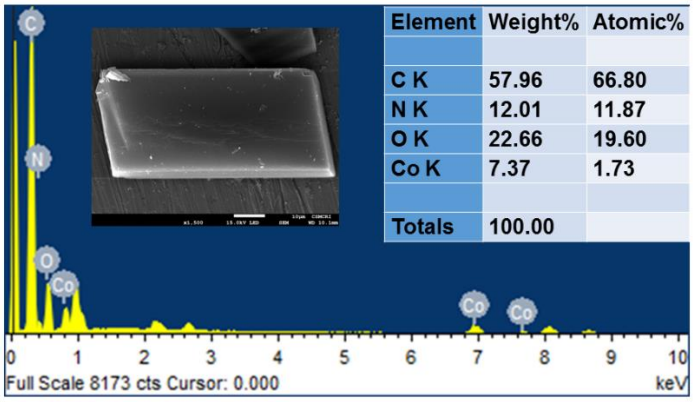

Element	Weight%	Atomic%
C K	57.96	66.80
N K	12.01	11.87
O K	22.66	19.60
Co K	7.37	1.73
Totals	100.00	

Fig. S3 FE-SEM image and EDX pattern of **CSMCRI-21**.

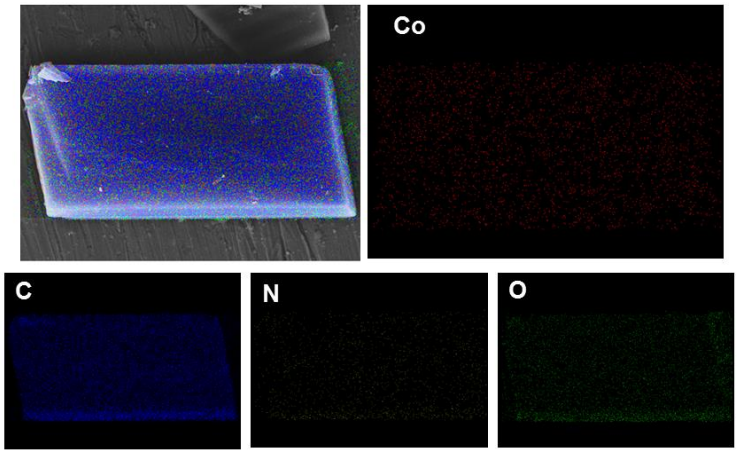

Fig. S4 Elemental mapping of **CSMCRI-21** revealing the coexistence of Co (red), C (blue), N (yellow) and O (green).

a)

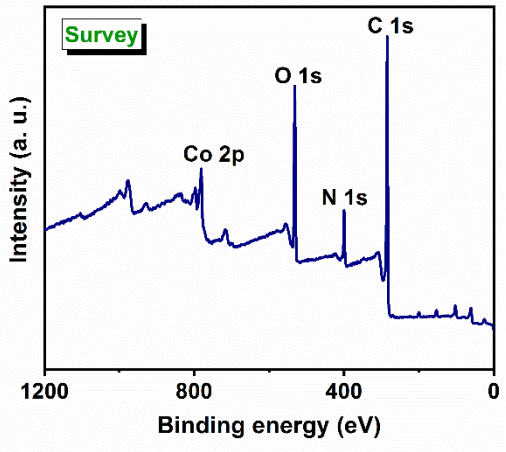

b)

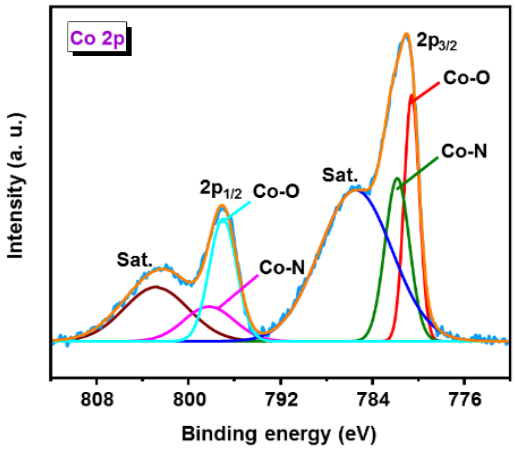

c)

d)

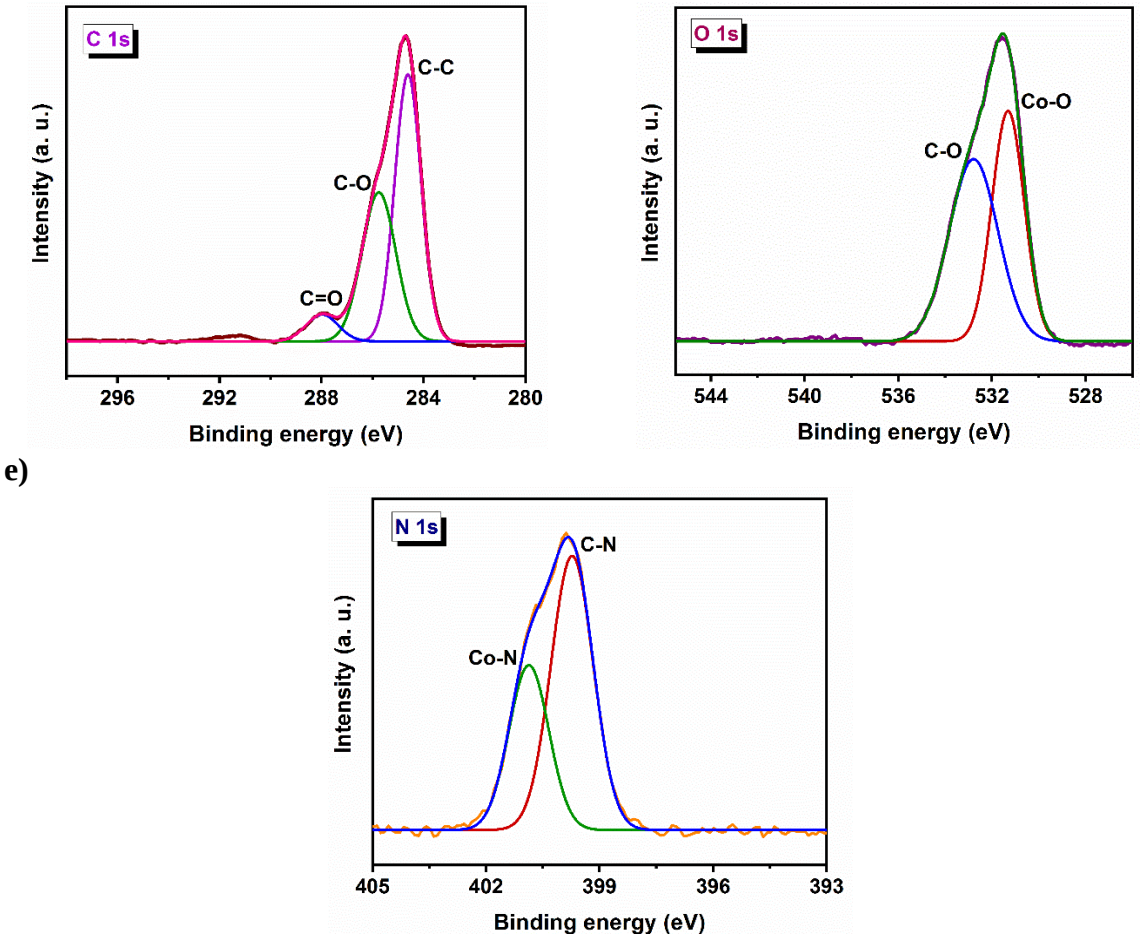

Fig. S5 (a) XPS survey spectrum of **CSMCRI-21**. High resolution XPS spectra of (b) Co 2p, (c) C 1s (d) O 1s and (e) N 1s for **CSMCRI-21**.

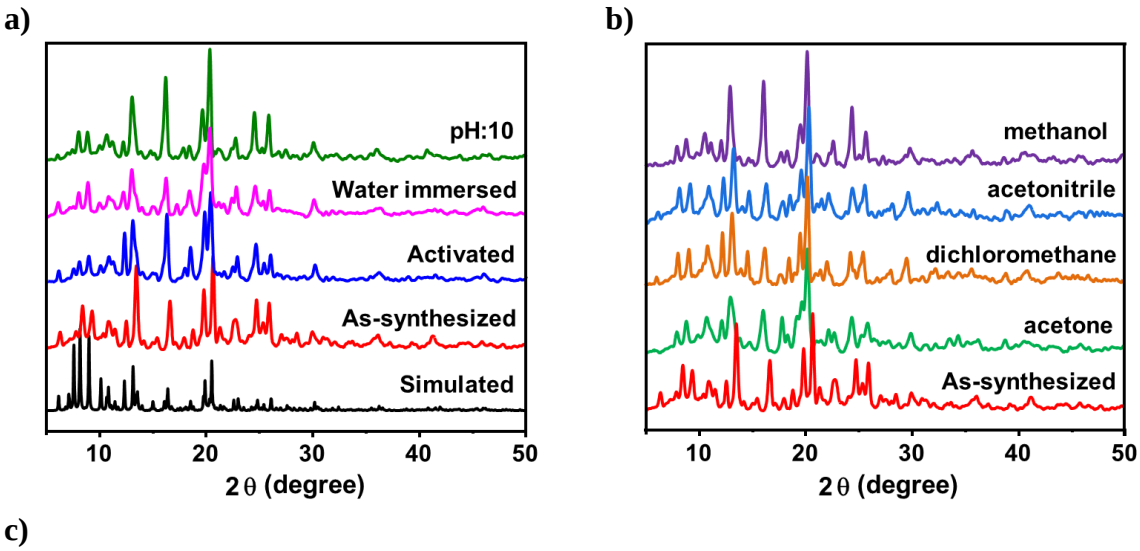

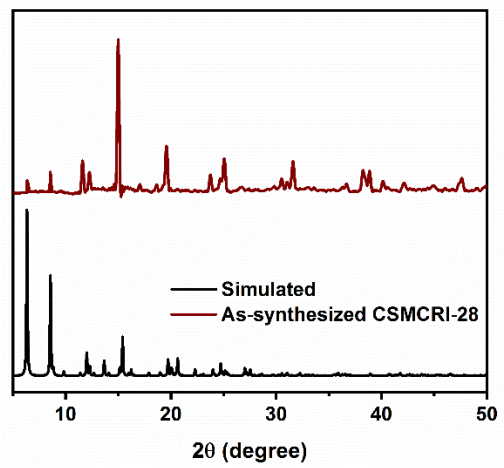

Fig. S6 PXRD pattern of **CSMCRI-21** in (a) several drastic condition and (b) diverse organic solvents. (c) Simulated and as-synthesized PXRD patterns of **CSMCRI-28**.

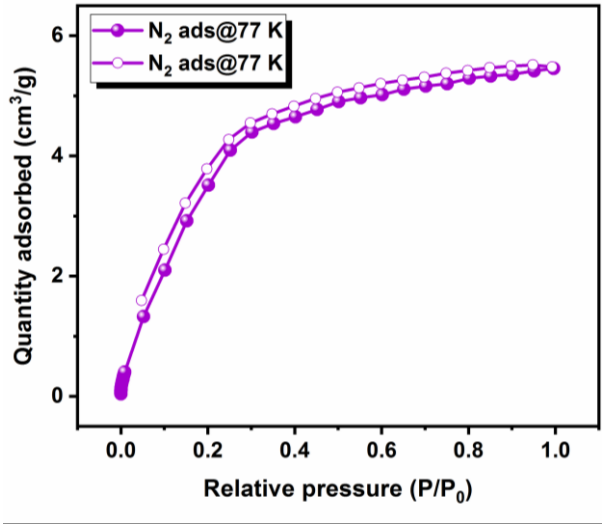

Fig. S7 N_2 adsorption isotherm of activated **CSMCRI-21** at 77 K.

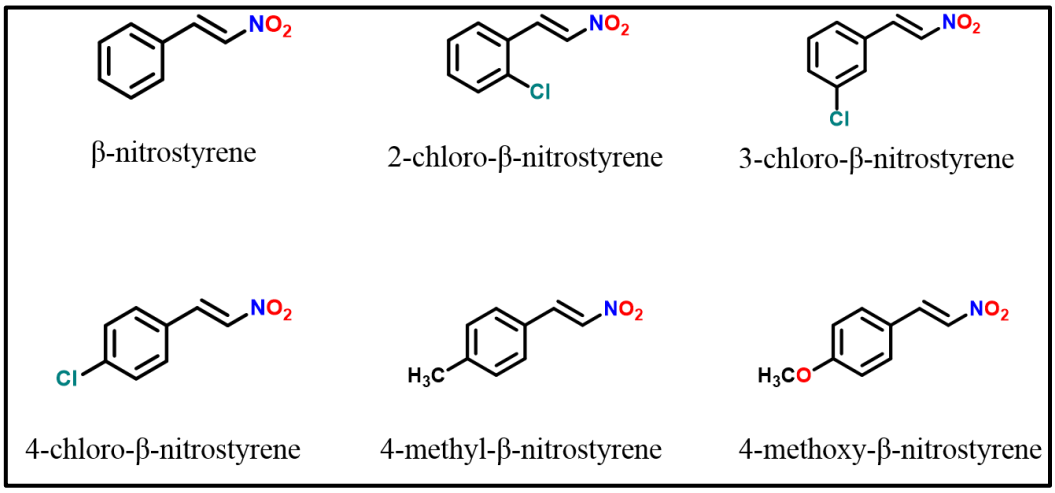

Fig. S8 Structure of differently substituted β-nitrostyrenes.

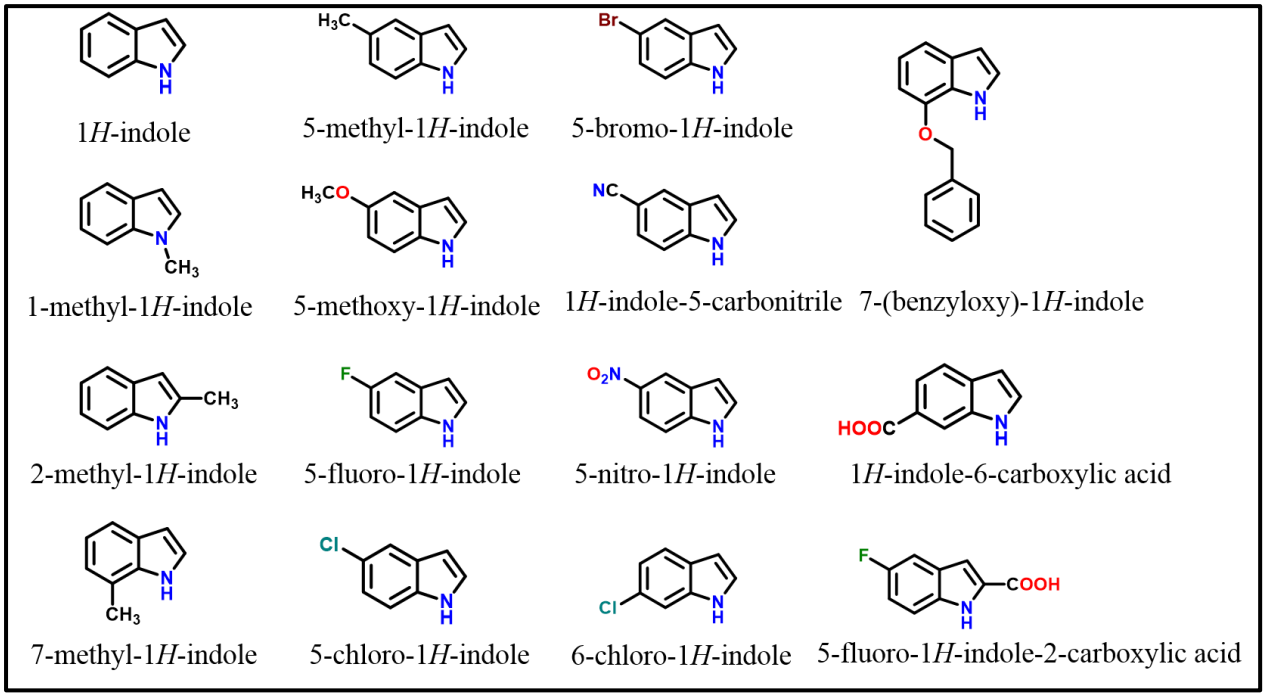

Fig. S9 Structure of differently substituted indoles.

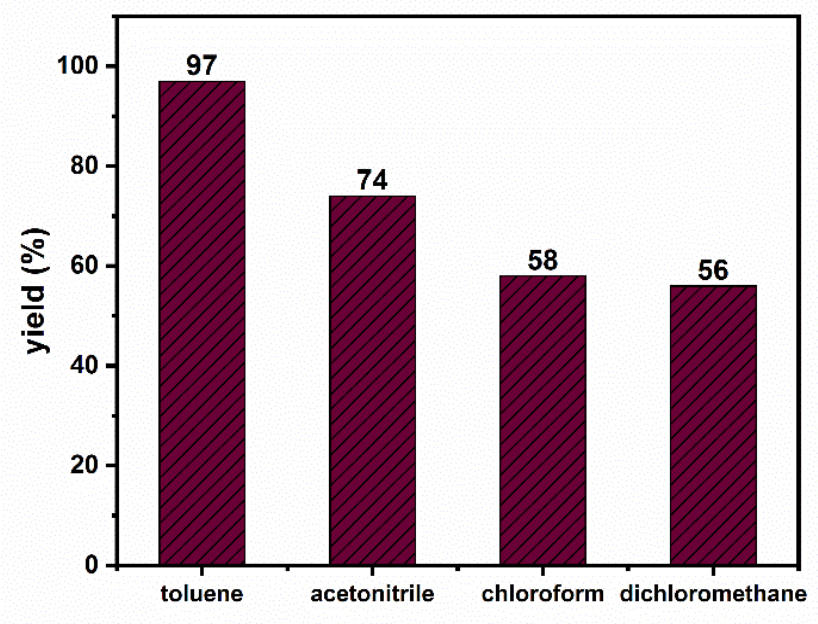

Fig. S10 Effect of solvents on yield for **21a** catalysed Friedel-Crafts reaction.

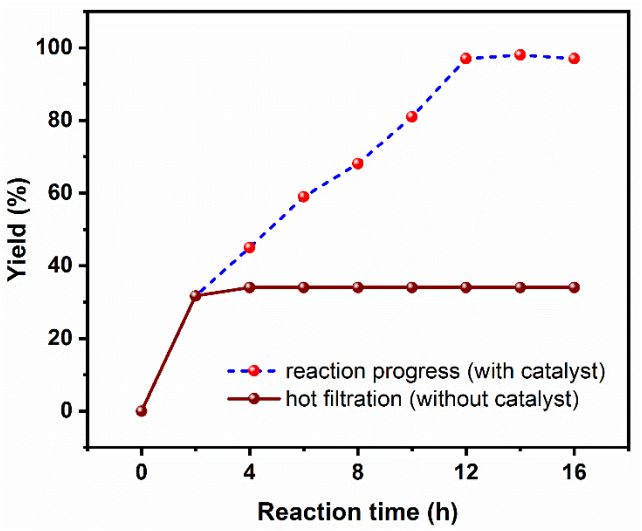

Fig. S11 Time-variable yield and hot-filtration test for the model reaction.

a) **b)**

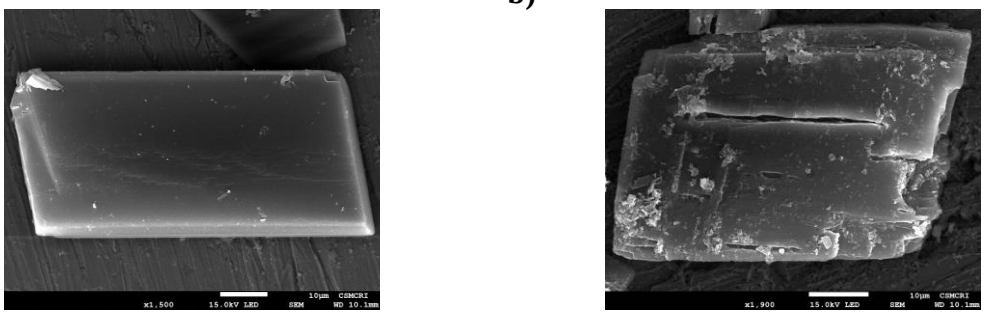

Fig. S12 FE-SEM image of (a) as-synthesized **CSMCRI-21** and (b) Ni^{2+}@**21a**, showing its unaltered morphology after Ni^{2+} incorporation.

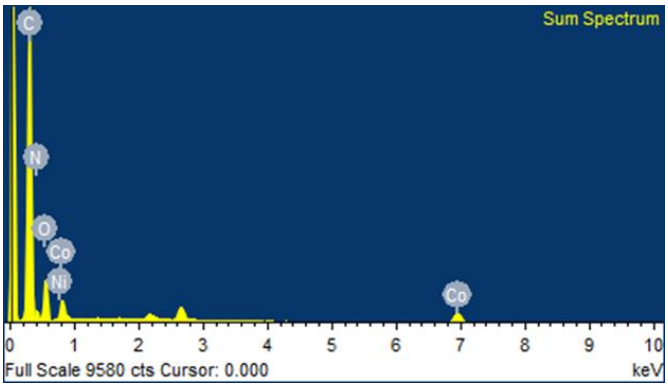

Fig. S13 SEM-EDX analysis of Ni^{2+}@**21a**, showing successful incorporation of Ni^{2+} within the MOF.

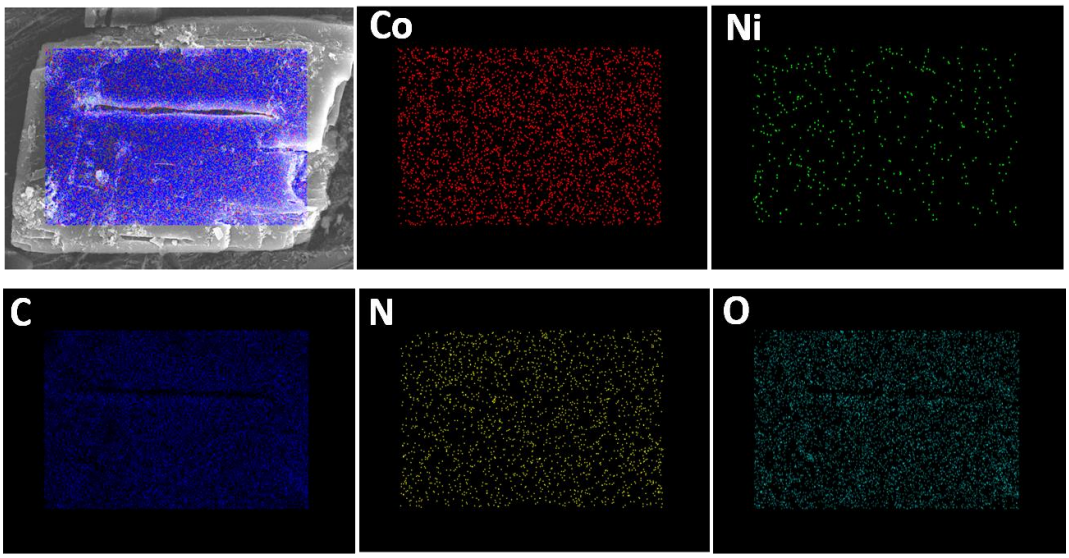

Fig. S14 Elemental mapping of Ni^{2+}@**21a**, showing uniform distribution of all the respective elements.

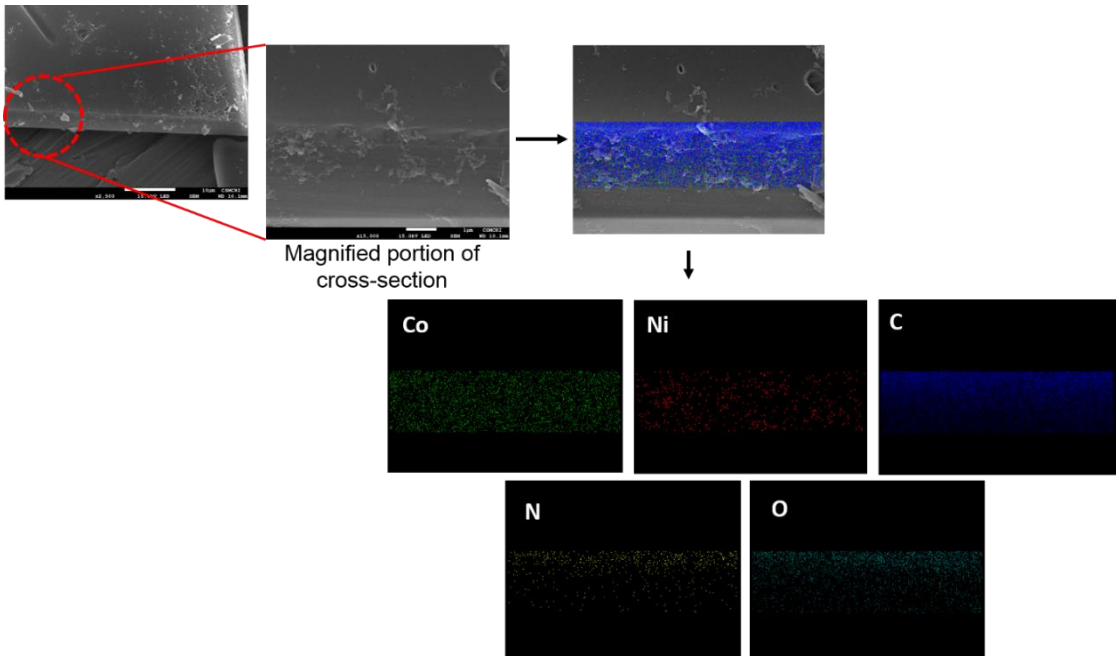

Fig. S15 elemental mapping of Ni in the cross-section of Ni^{2+}@**21a**.

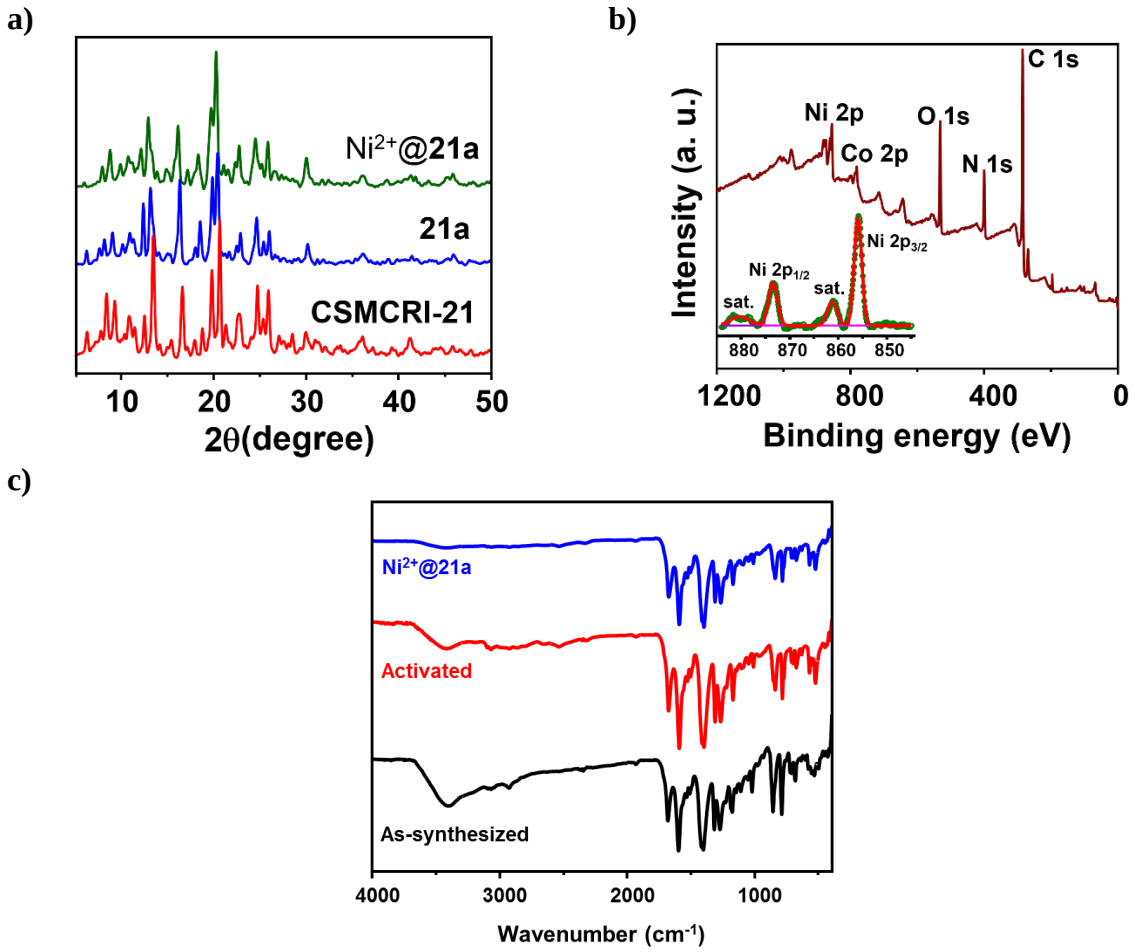

Fig. S16 (a) Comparison of PXRD patterns of Ni^{2+}@**21a** with as-synthesized and activated **CSMCRI-21**. (b) XPS survey spectrum of Ni^{2+}@**21a** (inset showing high-resolution XPS spectrum in the Ni 2p region). (c) FT-IR profile of the Ni^{2+}@**21a**, suggesting retention of structural integrity as well as successful incorporation of Ni^{2+}.

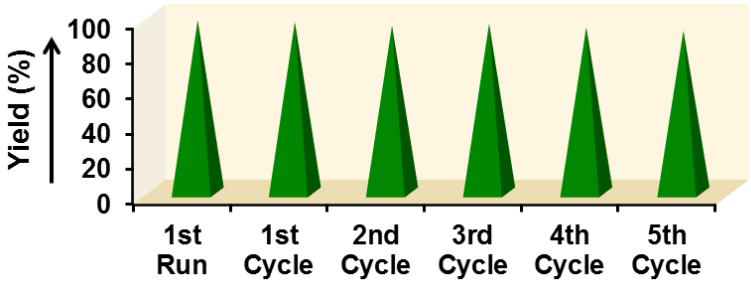

Fig. S17 Recyclability test of the catalyst up to five cycles in Friedel-Crafts alkylation, showing negligible loss in catalytic performance.

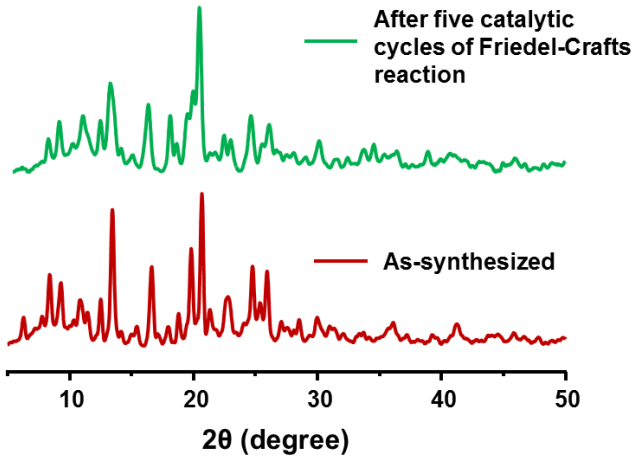

Fig. S18 PXRD pattern of the MOF, obtained after five catalytic cycles of Friedel-Crafts alkylation, corroborating retention of structural integrity during catalytic process.

a) **b)**

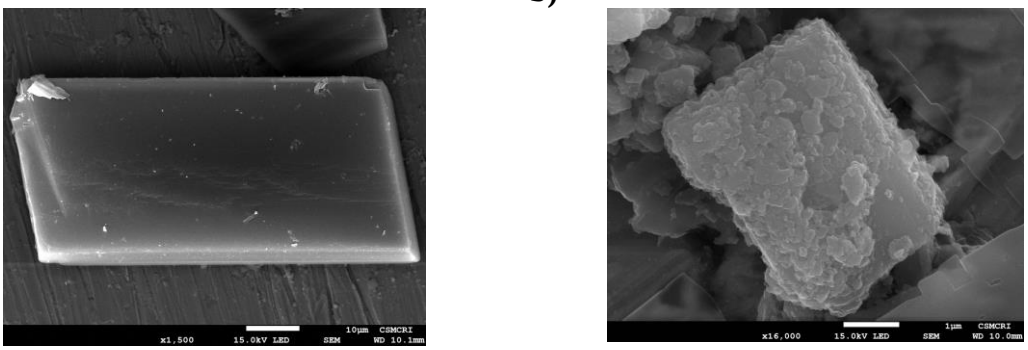

Fig. S19 FE-SEM images of (a) **CSMCRI-21** and (b) after five catalytic cycles of Friedel-Crafts alkylation, showing trivial change in block shaped morphology during catalysis.

a) **b)**

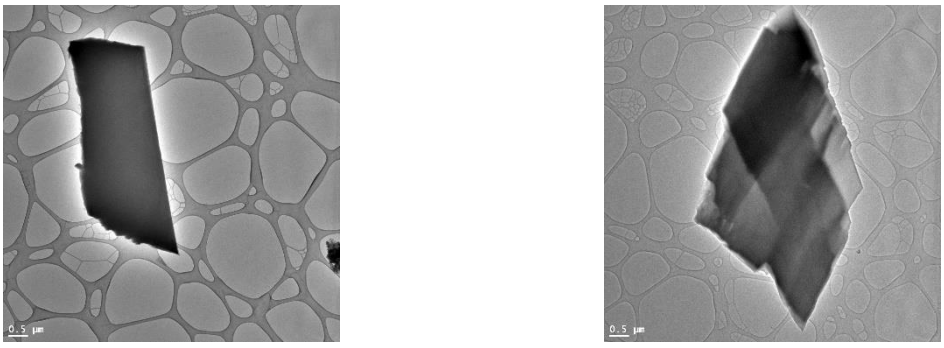

Fig. S20 TEM images of (a) **CSMCRI-21** and (b) after five catalytic cycles of Friedel-Crafts alkylation, showing trivial change in morphology during catalysis.

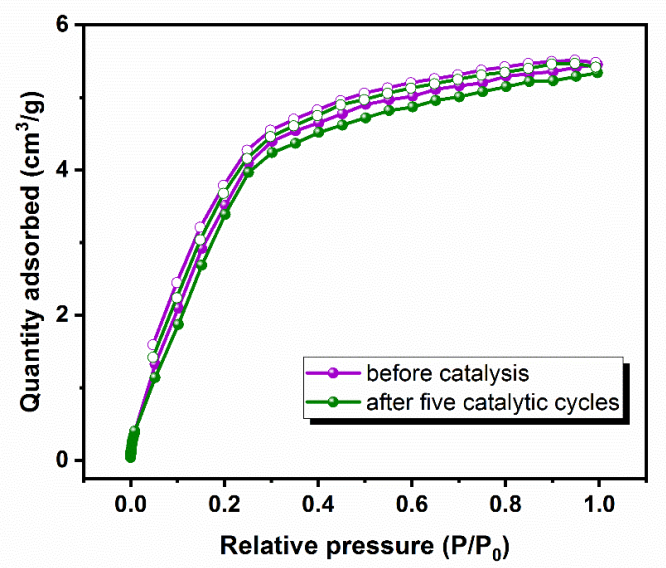

Fig. S21 N_2 adsorption isotherm of **21a** after five catalytic cycles of Friedel-Crafts reaction showing negligible deviation.

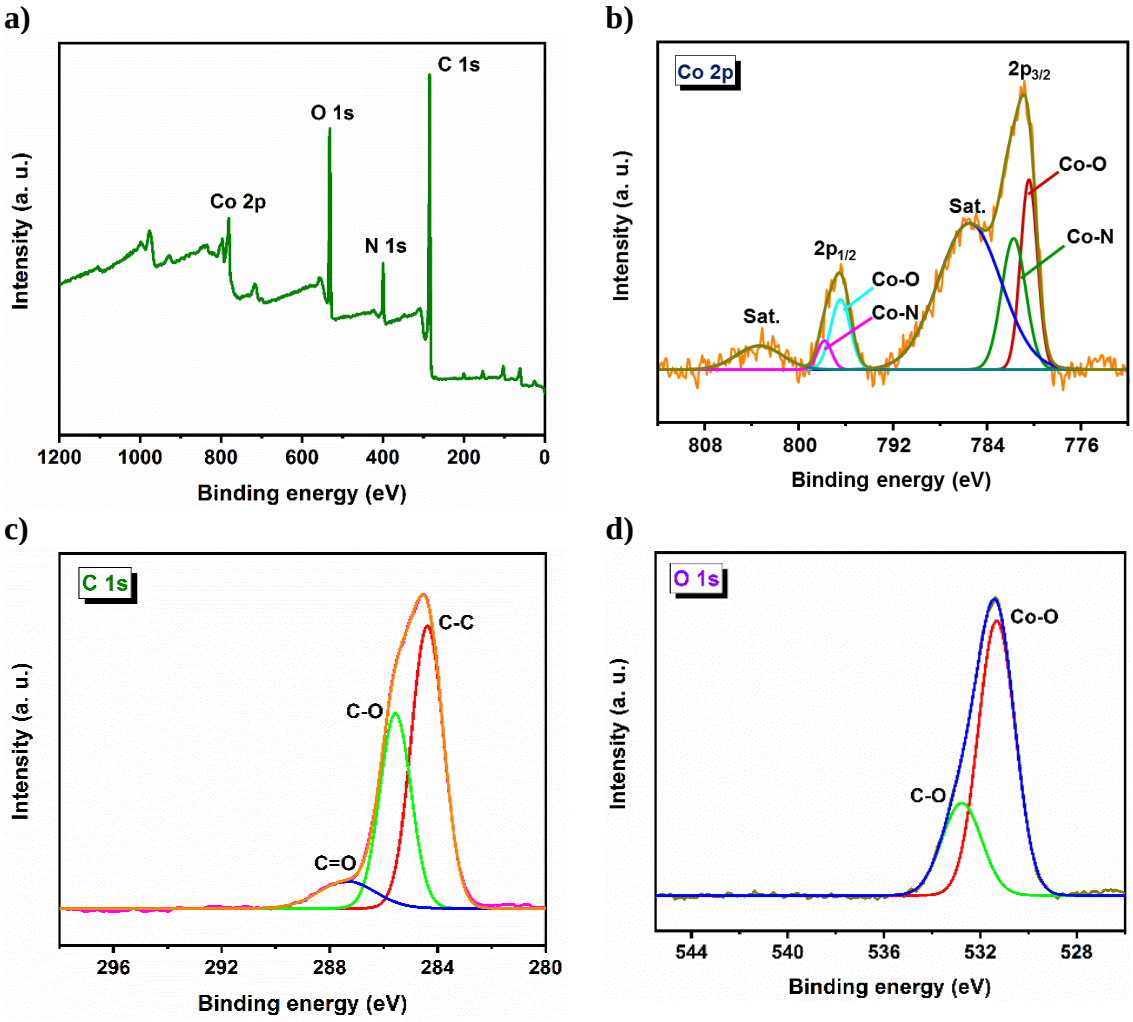

e)

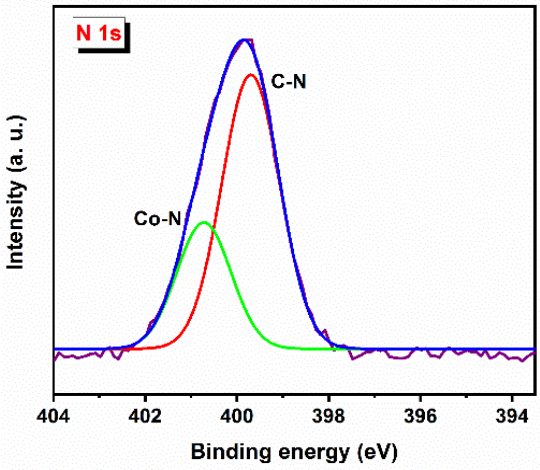

Fig. S22 (a) XPS survey spectrum, high-resolution XPS spectrum of (b) Co 2p, (c) C 1s, (d) N 1s and (e) O 1s after five catalytic cycles of Friedel-Crafts alkylation, showing trivial change in peak patterns to that of pristine catalyst **21a**.

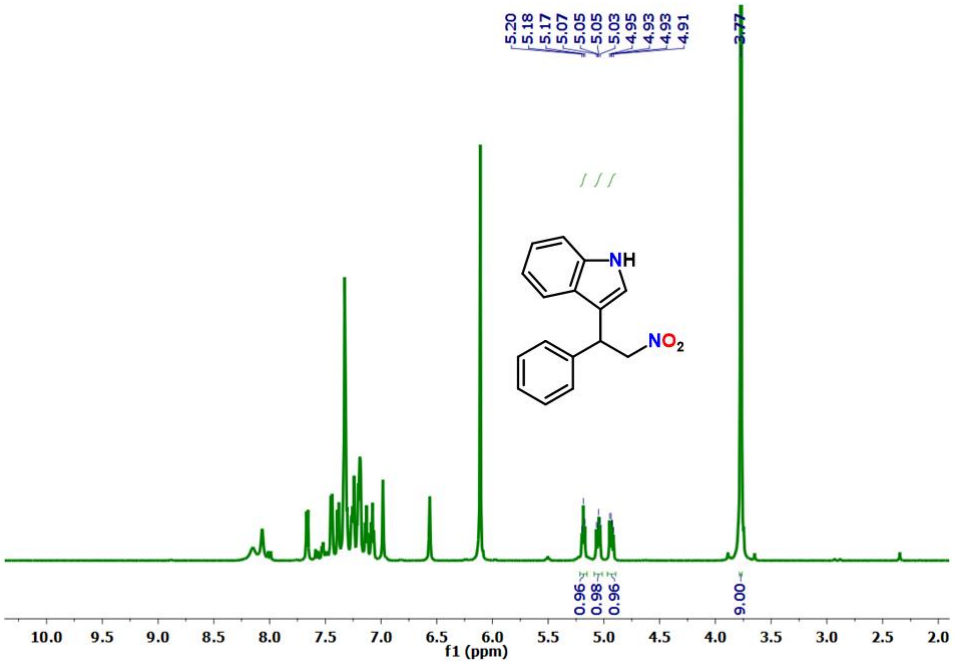

Fig. S23 ^{1}H NMR spectrum for **21a** catalysed Friedel-Crafts reaction between indole and β-nitrostyrene under optimized condition (Table 2, entry 1). 1,3,5-trimethoxybenzene was used as internal standard.

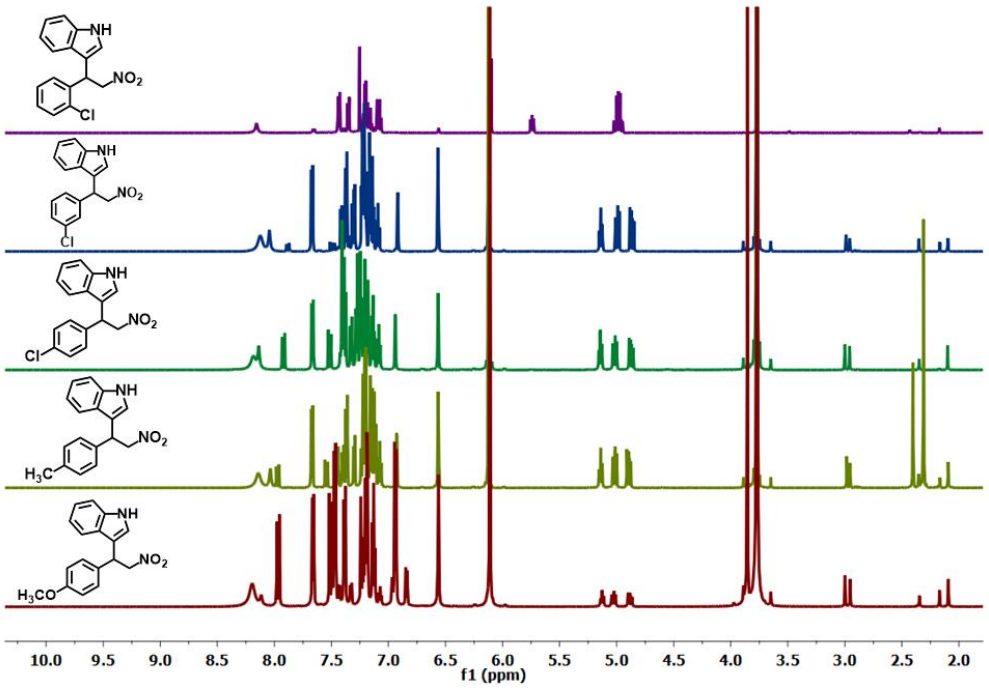

Fig. S24 ^{1}H NMR spectra for the substrate scope of β-nitrostyrene in the Friedel-Crafts alkylation reaction catalysed by **21a** (Table 2, entries 2-6). 1,3,5-trimethoxybenzene was used as internal standard.

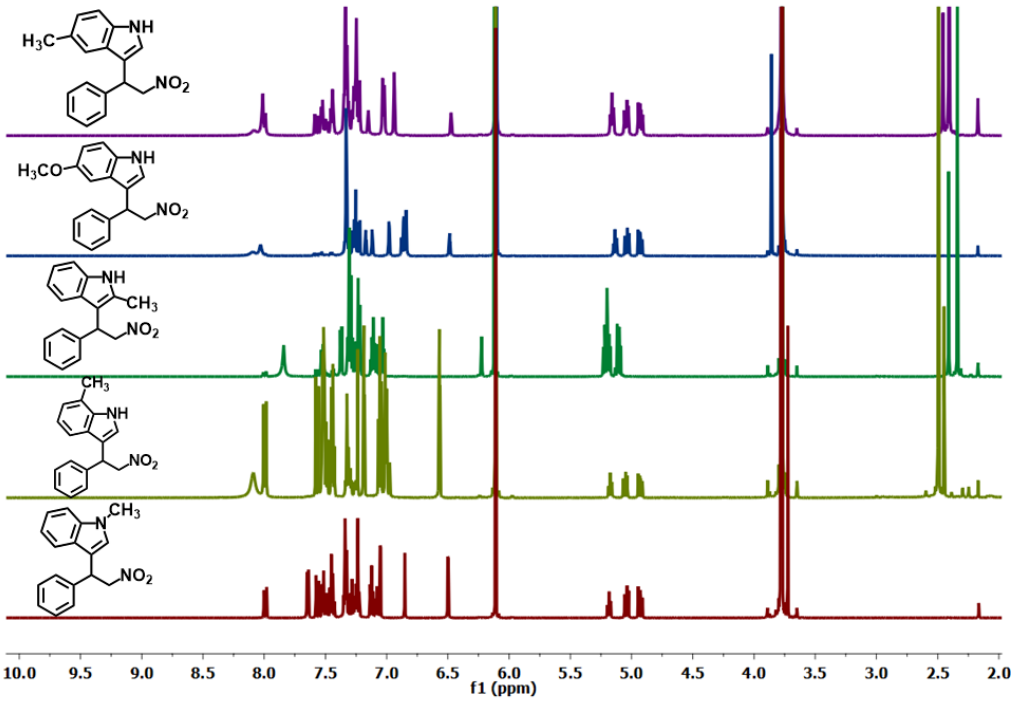

Fig. S25 ^{1}H NMR spectra for the substrate scope of electron donating indoles in Friedel-Crafts alkylation reaction catalysed by **21a** (Table 2, entries 7-10, and 18). 1,3,5-trimethoxybenzene was used as internal standard.

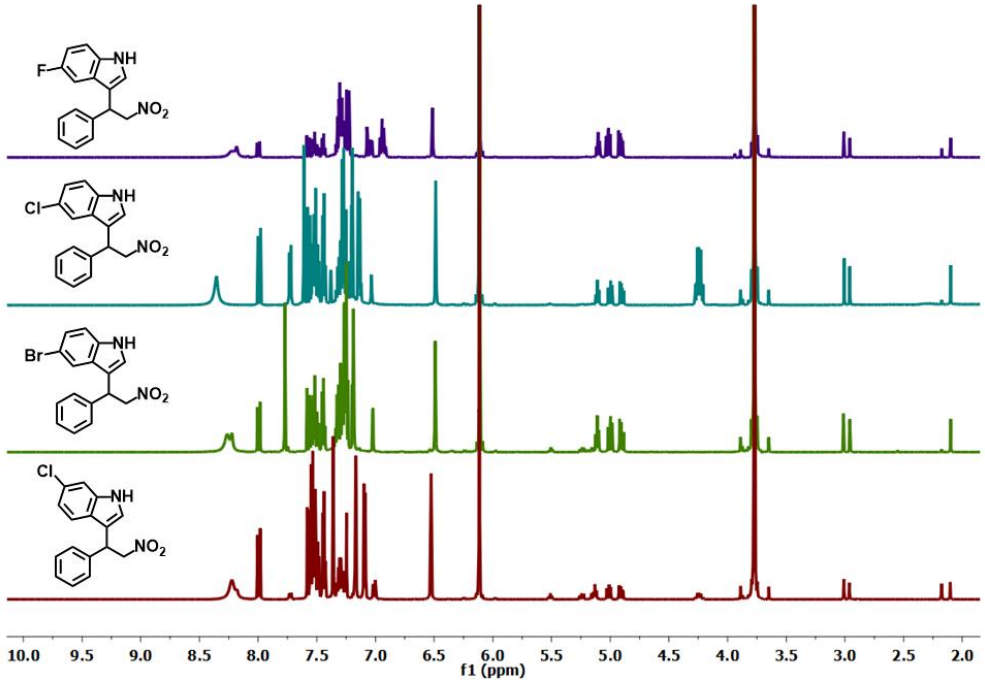

Fig. S26 ^{1}H NMR spectra for the substrate scope of electron withdrawing indole in Friedel-Crafts alkylation reaction catalysed by **21a** (Table 2, entries 11-14). 1,3,5-trimethoxybenzene was used as internal standard.

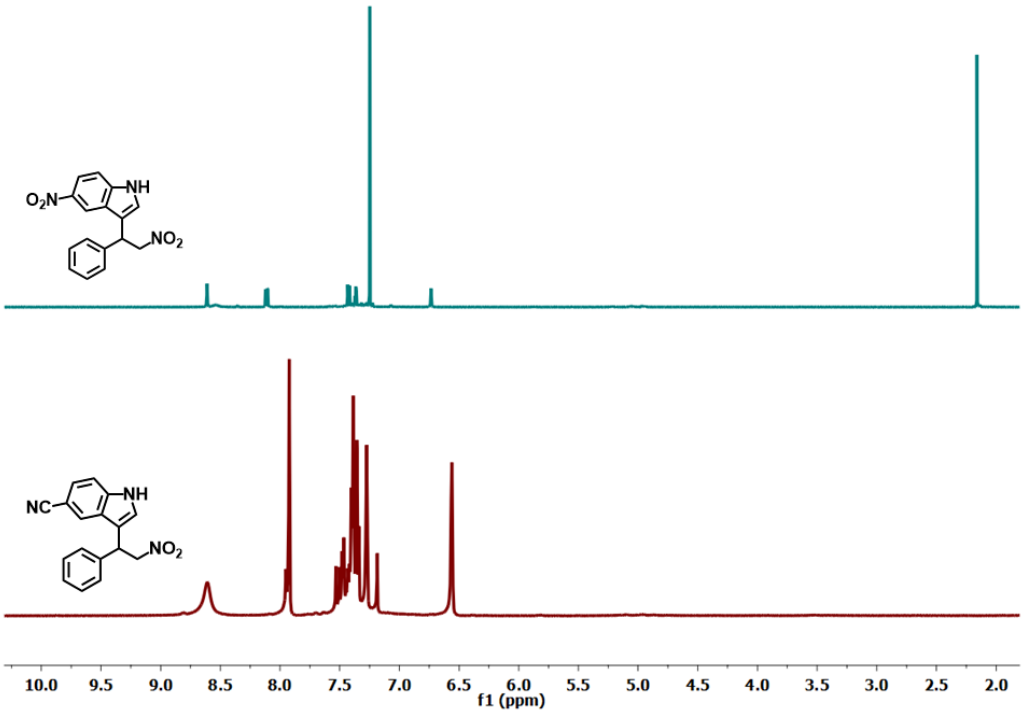

Fig. S27 ^{1}H NMR spectrum for **21a** catalysed Friedel-Crafts reaction between 5-nitro and 5-cyanoindole with β-nitrostyrene, respectively, under optimized condition (Table 2, entry 15 and 16).

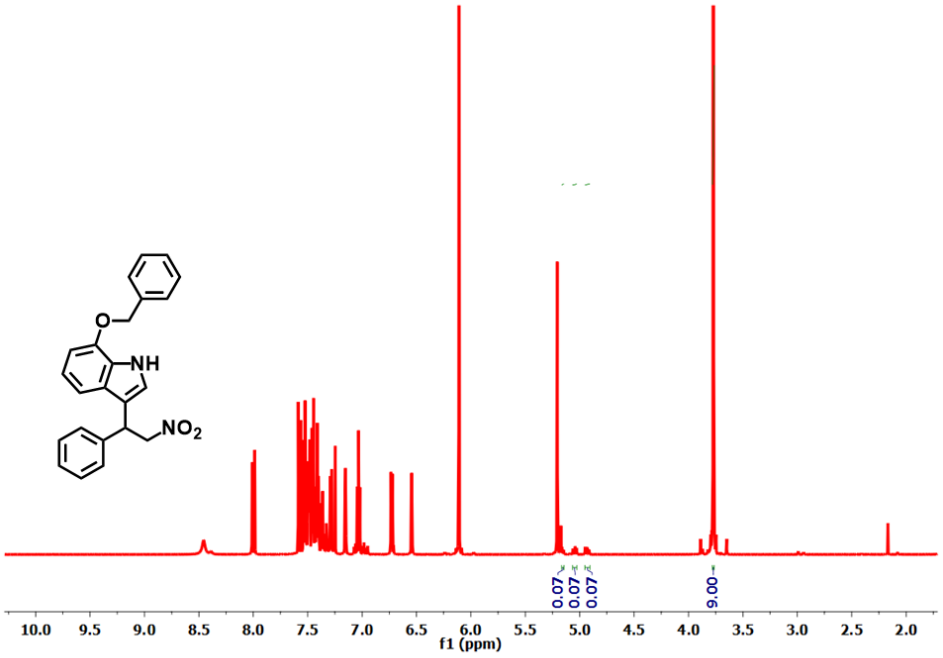

Fig. S28 ^{1}H NMR spectrum for **21a** catalysed Friedel-Crafts reaction between 7-benzyloxyindole and β-nitrostyrene under optimized condition (Table 2, entry 17). 1,3,5-trimethoxybenzene was used as internal standard.

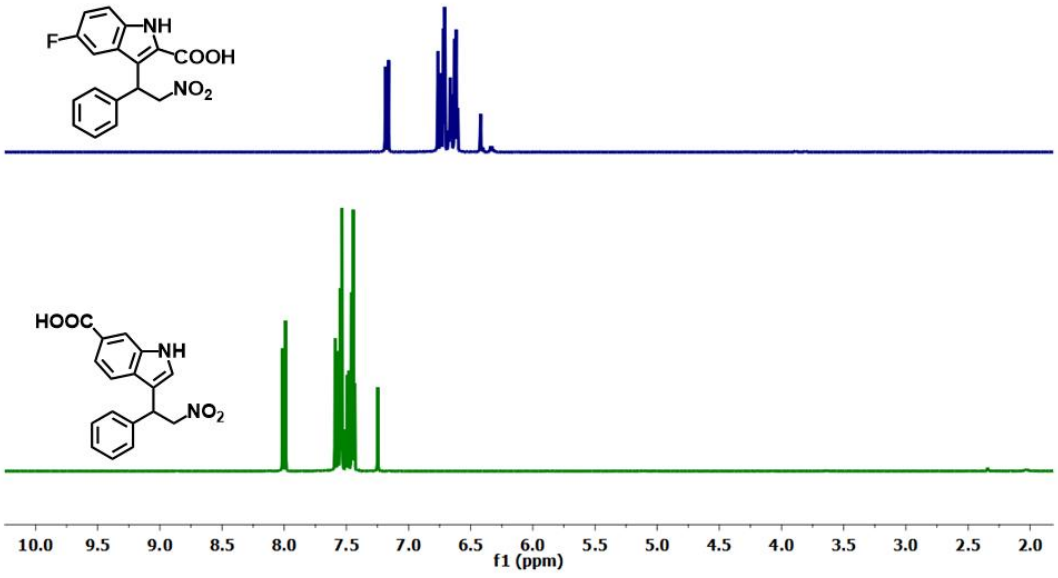

Fig. S29 ^{1}H NMR spectrum for **21a** catalysed Friedel-Crafts reaction between 5-fluoroindole-2-carboxylic acid and indole-6-carboxylic acid with β-nitrostyrene, respectively, under optimized condition (Table 2, entry 19 and 20).

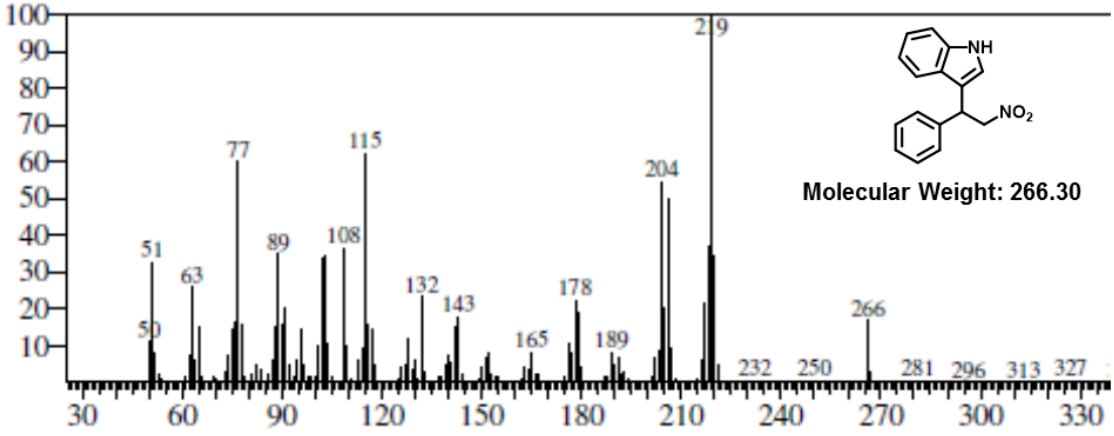

Fig. S30 GC-MS trace of 3-(2-nitro-1-phenylethyl)-1*H*-indole.

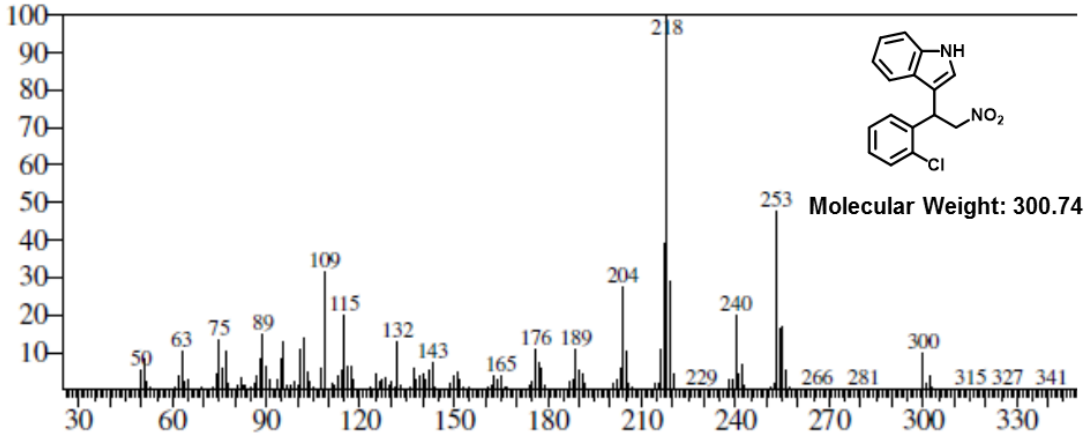

Fig. S31 GC-MS trace of 3-(1-(2-chlorophenyl)-2-nitroethyl)-1*H*-indole.

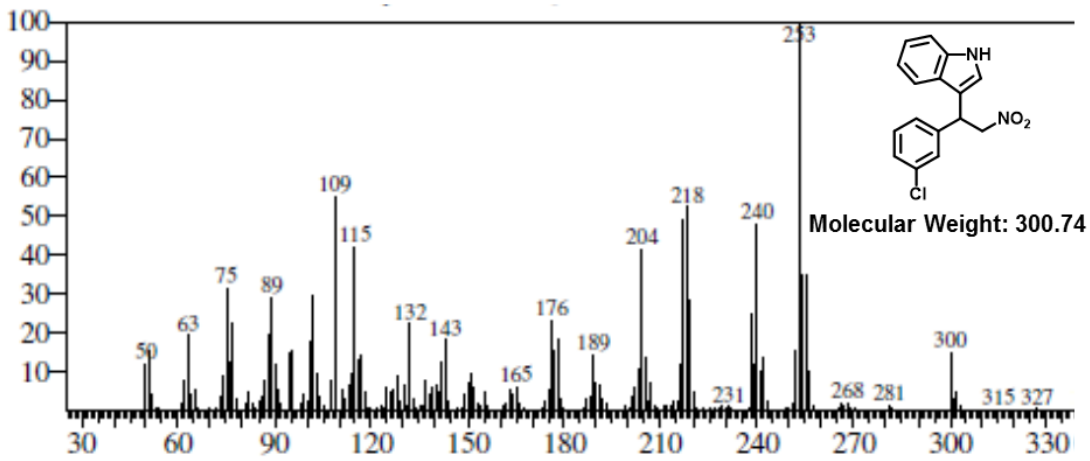

Fig. S32 GC-MS trace of 3-(1-(3-chlorophenyl)-2-nitroethyl)-1*H*-indole.

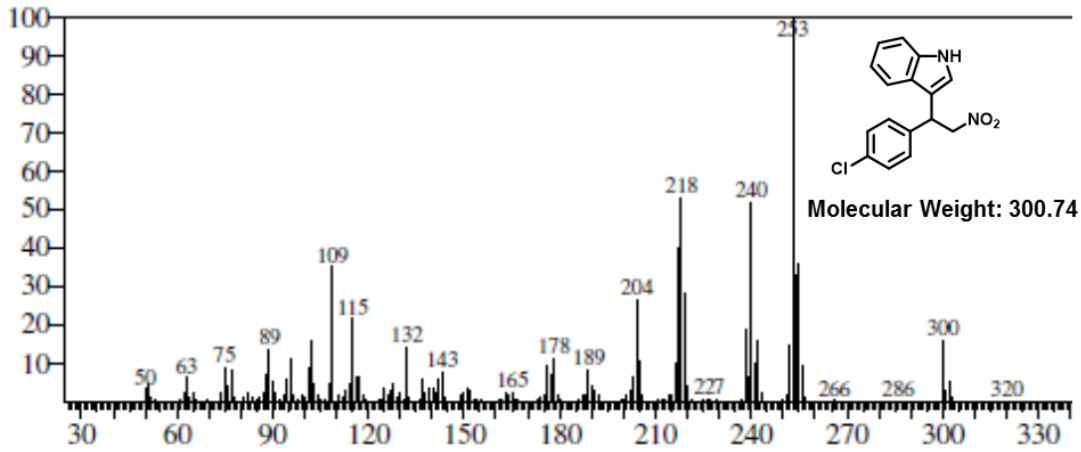

Fig. S33 GC-MS trace of 3-(1-(4-chlorophenyl)-2-nitroethyl)-1*H*-indole.

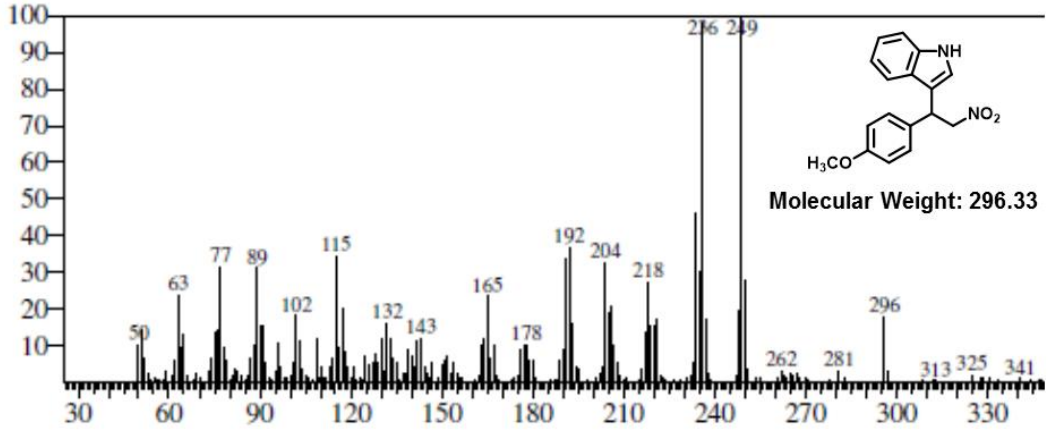

Fig. S34 GC-MS trace of 3-(1-(4-methoxyphenyl)-2-nitroethyl)-1*H*-indole.

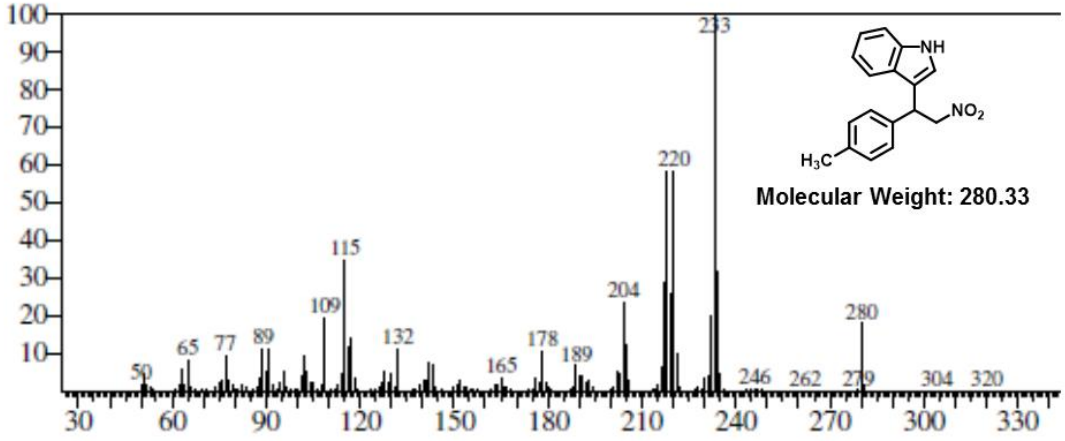

Fig. S35 GC-MS trace of 3-(2-nitro-1-(p-tolyl)ethyl)-1*H*-indole.

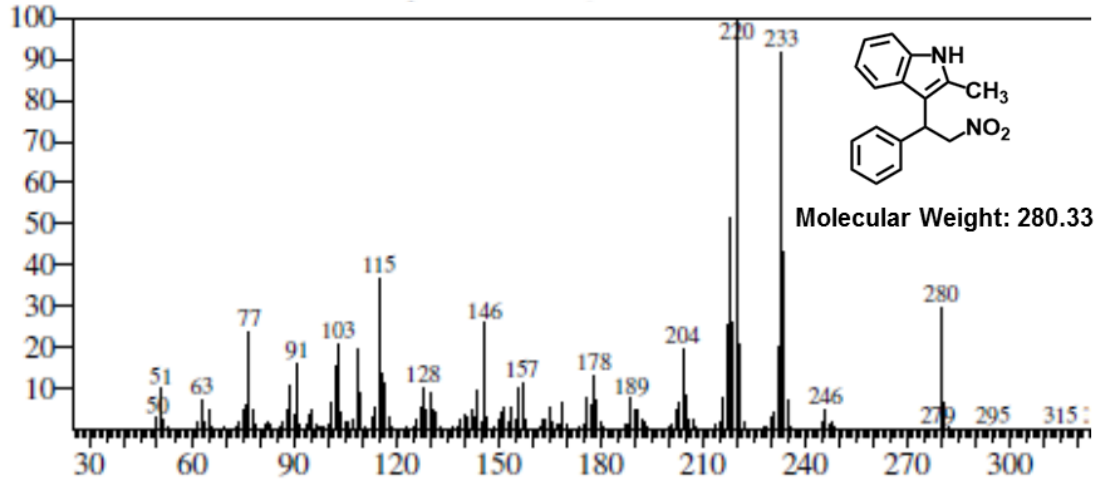

Fig. S36 GC-MS trace of 2-methyl-3-(2-nitro-1-phenylethyl)-1*H*-indole.

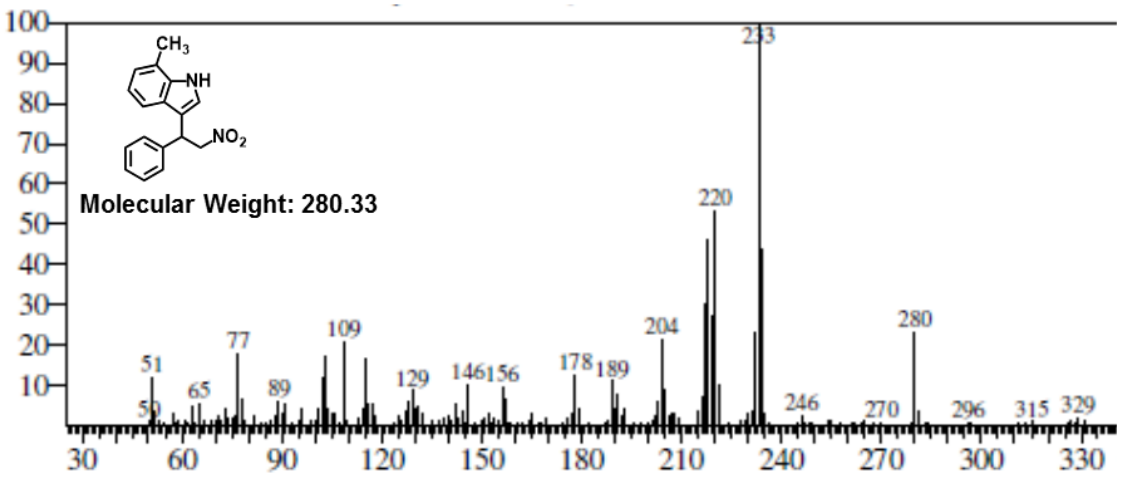

Fig. S37 GC-MS trace of 7-methyl-3-(2-nitro-1-phenylethyl)-1*H*-indole.

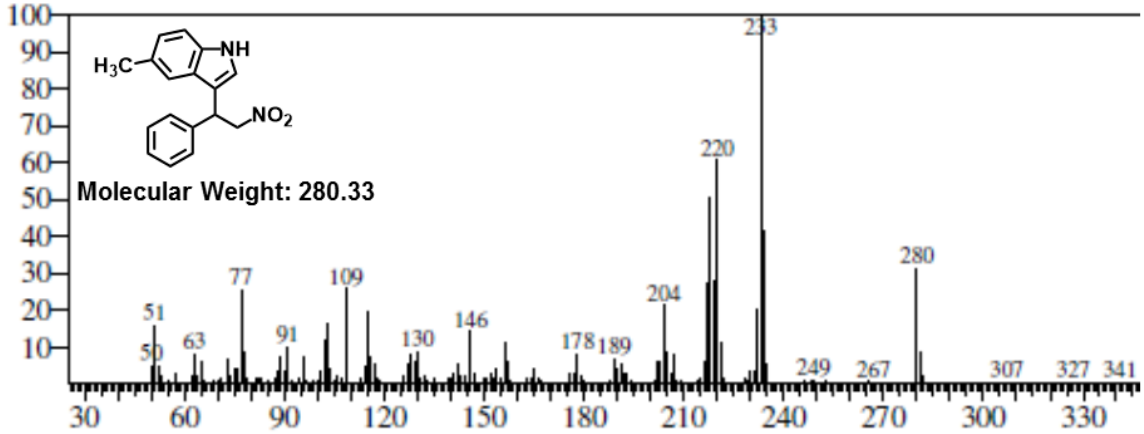

Fig. S38 GC-MS trace of 5-methyl-3-(2-nitro-1-phenylethyl)-1*H*-indole.

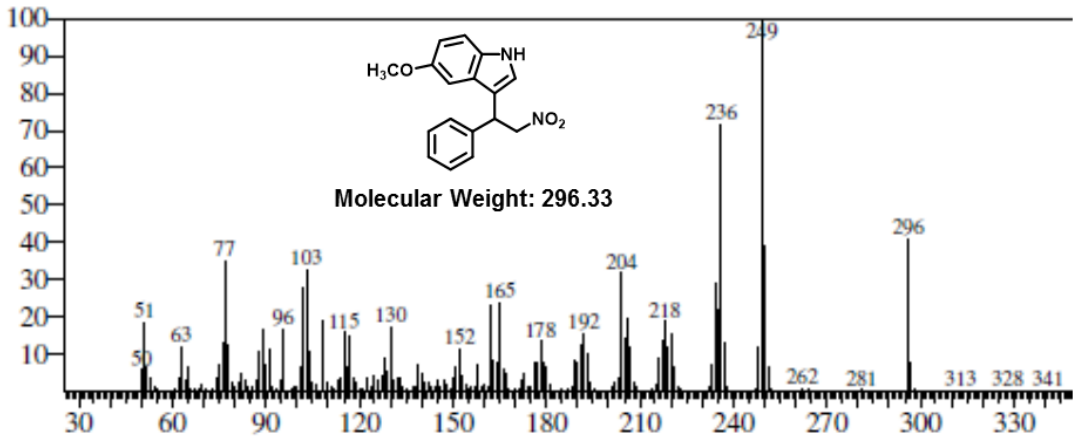

Fig. S39 GC-MS trace of 5-methoxy-3-(2-nitro-1-phenylethyl)-1*H*-indole.

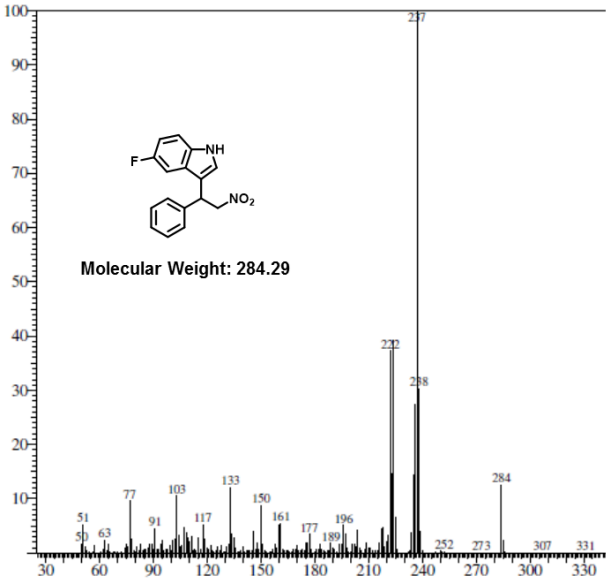

Fig. S40 GC-MS trace of 5-fluoro-3-(2-nitro-1-phenylethyl)-1*H*-indole.

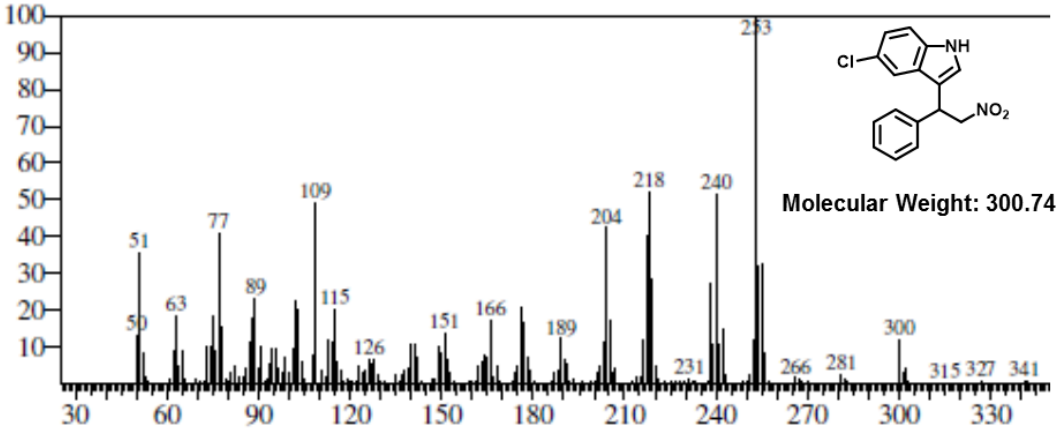

Fig. S41 GC-MS trace of 5-chloro-3-(2-nitro-1-phenylethyl)-1*H*-indole.

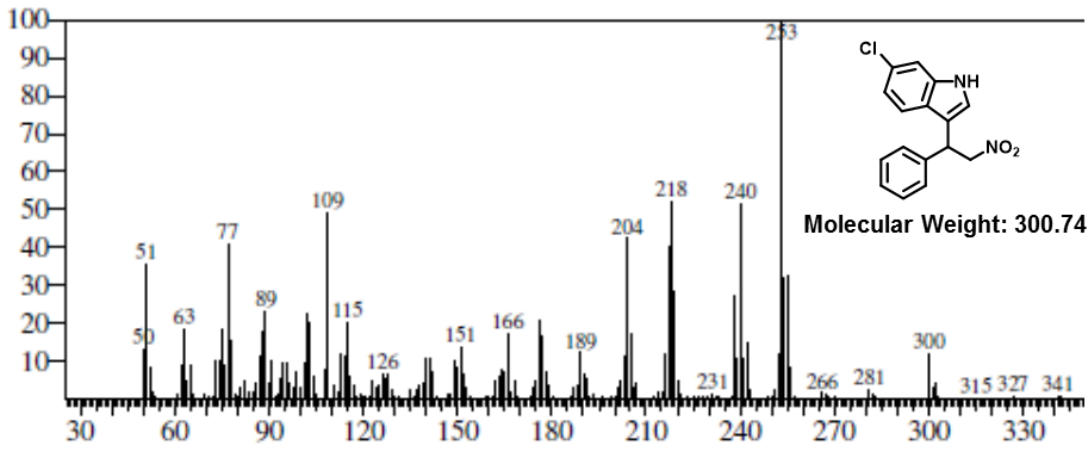

Fig. S42 GC-MS trace of 6-chloro-3-(2-nitro-1-phenylethyl)-1*H*-indole.

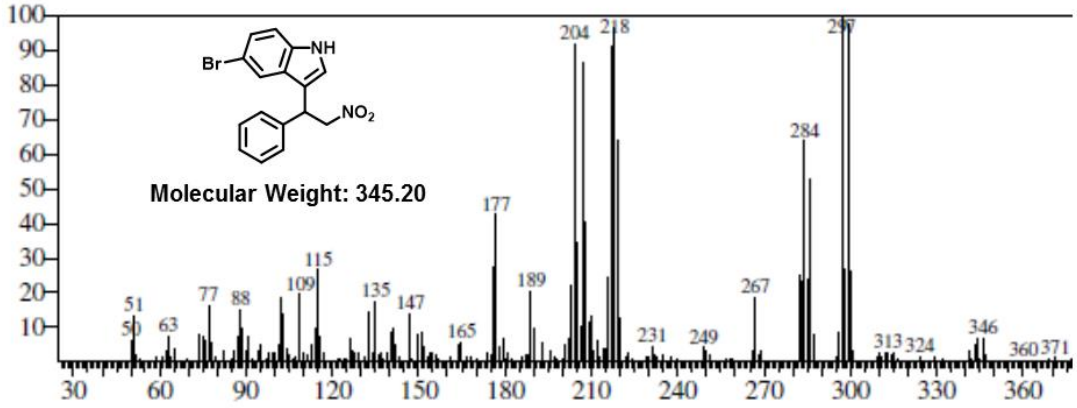

Fig. S43 GC-MS trace of 5-bromo-3-(2-nitro-1-phenylethyl)-1*H*-indole.

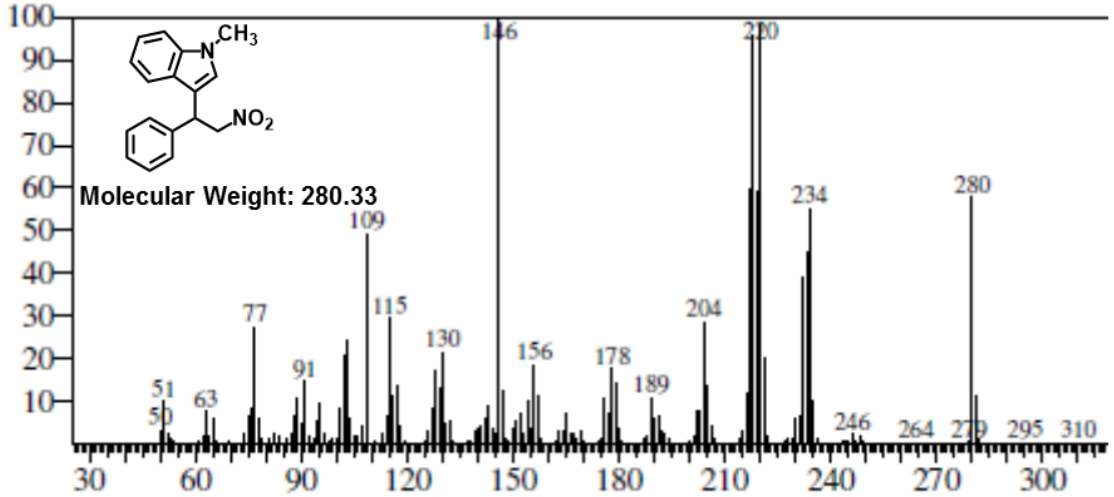

Fig. S44 GC-MS trace of *N*-methyl-3-(2-nitro-1-phenylethyl)-1*H*-indole.

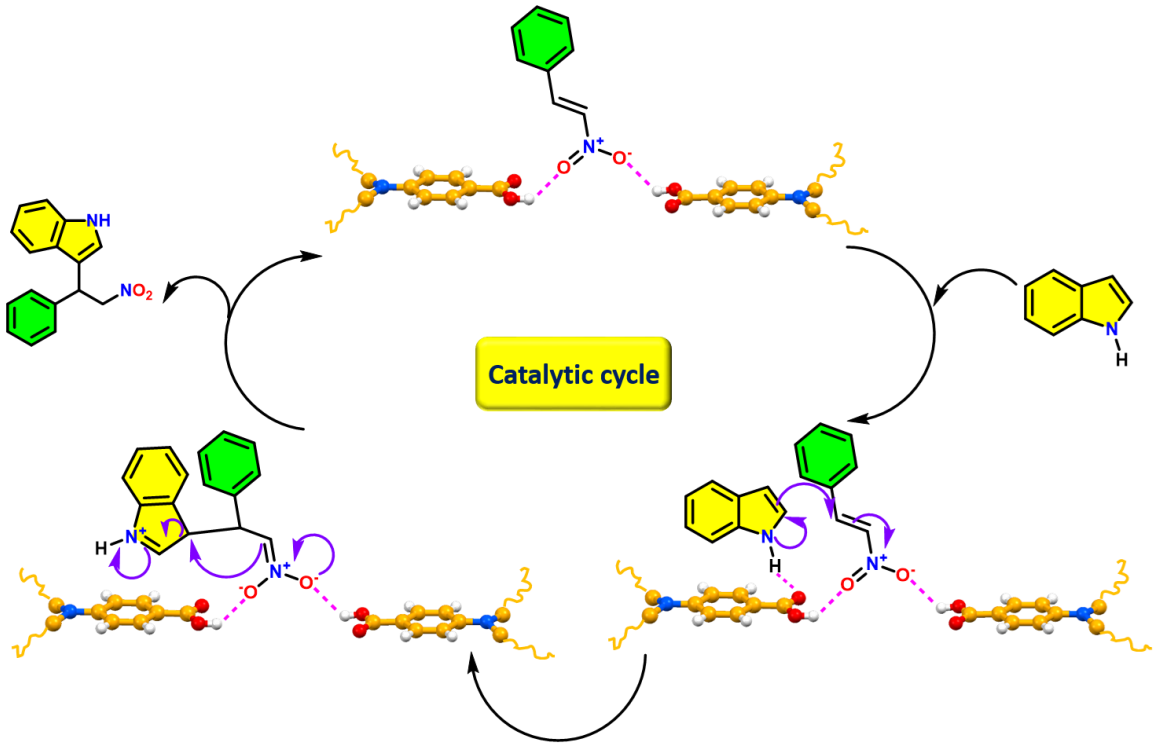

Fig. S45 Plausible reaction mechanism of **21a** catalysed hydrogen-bond-donating Friedel-Crafts alkylation.

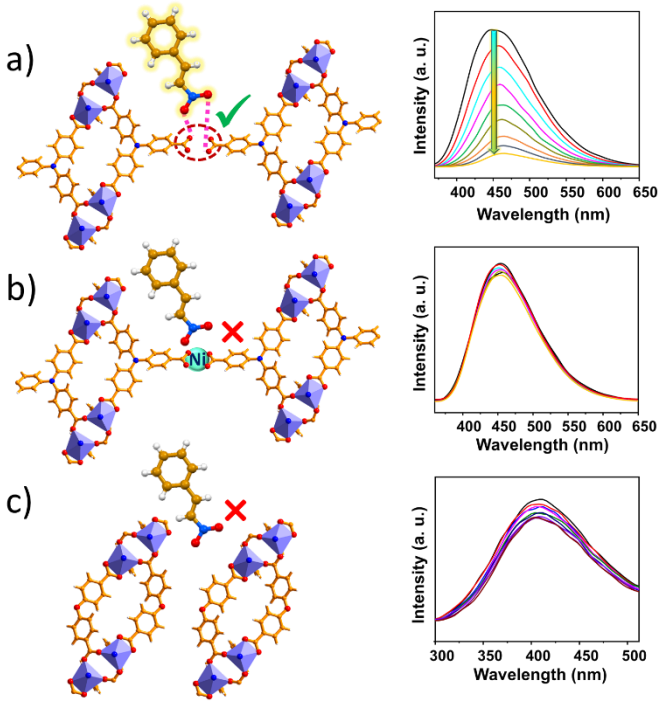

Fig. S46 Schematic validation of presence/ absence of two-point H-bonding between electrophile and –COOH moieties from luminescence change in (a) **21a** (b) Ni^{2+}@**21a** and (c) **28a** by β-nitrostyrene (160 µL).

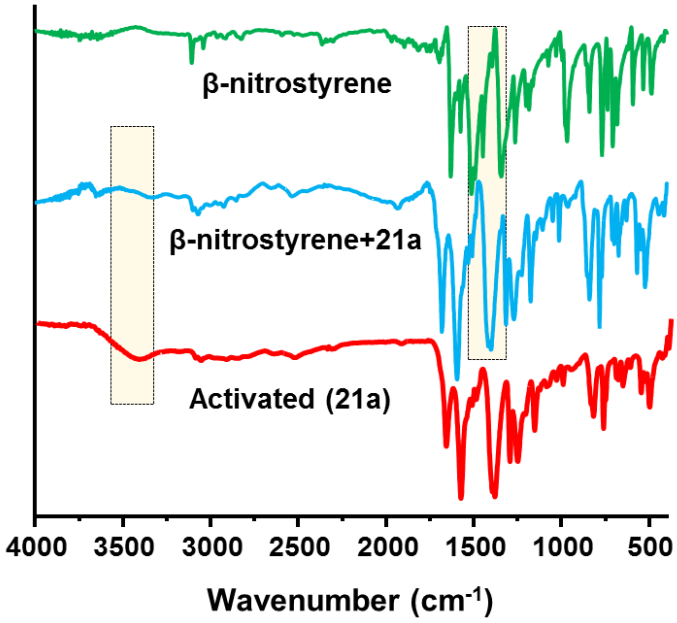

Fig. S47 FT-IR profile of the adduct of β-nitrostyrene and **21a**, showing decrease in COOH band intensity and shifts of N-O vibrations, which corroborates H-bonding interaction between free –COOH groups of **21a** and $–NO_2$ group of electrophile.

Table S1. Crystal data and refinement parameters for **CSMCRI-21**

Identification code	**CSMCRI-21**
Empirical formula	$C_{92}H_{60}Co_3N_{16}O_{18}$
Formula weight	1854.40
Temperature/K	302.15
Crystal system	triclinic
Space group	P-1
a/Å	13.3607(9)
b/Å	14.7831(9)
c/Å	25.4340(18)
α/°	97.603(2)
β/°	97.392(2)
γ/°	100.151(2)
Volume/$Å^3$	4841.6(6)
Z	2
$\rho_{calc}g/cm^3$	1.2719

μ/mm^{-1}	0.579
F(000)	1901.0
Crystal size/mm^3	0.467 × 0.19 × 0.08
Radiation	Mo Kα (λ = 0.71073)
2Θ range for data collection/°	4.58 to 56.74
Index ranges	$-17 \leq h \leq 17$, $-19 \leq k \leq 19$, $-33 \leq l \leq 33$
Reflections collected	137213
Independent reflections	24065 [R_{int} = 0.0819, R_{sigma} = 0.0691]
Data/restraints/parameters	24065/0/1162
Goodness-of-fit on F^2	1.079
Final R indexes [I>=2σ (I)]	R_1 = 0.0611, wR_2 = 0.1735
Final R indexes [all data]	R_1 = 0.1132, wR_2 = 0.2178

Determination of formula & solvent composition of CSMCRI-21 from PLATON Squeeze and Thermogravimetric analysis data:

From the TGA plot of as-synthesized **CSMCRI-21**, the observed mass loss is 15.19 %

From PLATON Squeeze program void electron count / unit cell comes out to be 190.5

As DMF and water were used as solvents during the synthesis of the MOF, so the void space should be occupied by these lattice solvent molecules.

Now, formula of the asymmetric unit excluding guest solvents is $[Co_3(TCA)_3(dpa)_3]$, and mass of this asymmetric unit is 1854.4

Table S2. Number of electrons and molecular mass of guest molecules associated with **CSMCRI-21** for determination of solvent composition and molecular formula

	Dimethyl formamide (DMF)	Water
No. of electrons	40	10
mass	73	18

Considering the above mentioned number of electrons, the best possible combination of solvent molecules for **CSMCRI-21** could be $[Co_3(TCA)_3(dpa)_3]\cdot 3DMF\cdot 7H_2O$

The total number of electrons contributed by lattice solvent molecules will be [(40×3) + (10×7)] = 190, which is in complete agreement with the PLATON result and thus validates the above formula.

The aforementioned combination was further cross-checked from TGA analysis.

Mass loss due to lattice solvents is [(73×3) + (18×7)] = 345

Therefore, total mass of **CSMCRI-21** including lattice solvents is (1854.4+345) = 2199.4

So mass loss due to lattice water molecules is [(126/2199.4) ×100] % = 5.72 %

Mass loss due to lattice DMF molecules is [(219/2199.4) ×100] % = 9.95 %

So total mass loss for solvents is (5.72+9.95) % = 15.67 %, which is in good agreement with that of the TGA result.

Table S3. Crystal data and refinement parameters for **CSMCRI-28**

Identification code	**CSMCRI-28**
Empirical formula	$C_{24}H_{16}CoN_4O_5$
Formula weight	499.35
Temperature/K	273.15
Crystal system	triclinic
Space group	P-1
a/Å	9.081(4)
b/Å	11.007(6)
c/Å	14.835(7)
α/°	70.42(2)
β/°	84.50(2)
γ/°	82.93(2)
Volume/Å^3	1384.1(12)
Z	2
ρ_{calc}g/cm^3	1.1980
μ/mm^{-1}	0.656
F(000)	510.9
Radiation	Mo Kα (λ = 0.71073)
2Θ range for data collection/°	3.94 to 61.46
Index ranges	-12 ≤ h ≤ 13, -15 ≤ k ≤ 15, -21 ≤ l ≤ 21
Reflections collected	94181
Independent reflections	8570 [R_{int} = 0.0804, R_{sigma} = 0.0382]
Data/restraints/parameters	8570/0/307

Goodness-of-fit on F^2	1.087
Final R indexes [I>=2σ (I)]	R_1 = 0.0413, wR_2 = 0.1278
Final R indexes [all data]	R_1 = 0.0603, wR_2 = 0.1509

Table S4. A comparison of catalytic performance of activated **CSMCRI-21** to that of other MOF materials in Friedel-Crafts alkylation reaction

Entry	MOF	Reaction Condition	Yield (%)	References
1.	$[Zn_2(azdc)_2(L)_2]\cdot 2DMF\cdot 2.5EtOH\cdot 3.5H_2O$	60 °C/ acetonitrile/5 mol%/12 h	97	*Inorg. Chem.* **2023**, 62, 871-884
2.	$[Cd_3(TCA)_2\boldsymbol{L}(H_2O)]\cdot 2DMA\cdot 10H_2O$	60 °C/toluene/10 mol%/16 h	100	*Inorg. Chem. Front.*, **2022**, *9*, 1897–1911
3.	UiO-67-Urea	70 °C/toluene/10 mg/24 h	97	*Inorg. Chem.* **2019**, *58*, 5163−5172
4.	$\{[Zn_2(2\text{-}BQBG)(BDC)_2]\cdot 10H_2O\}_n$	35 °C/DCM/3 mol%/12 h	100	*ACS Catal.* **2019**, *9*, 3165−3173
5.	$[Zn_4O(L_2)(DMF)_2]\cdot 3DMF$	60 °C/toluene/22 mol%/24 h	90	*ChemCatChem* **2017**, *9*, 1172– 1176
6.	Cu(dbda)	50 °C/ chloroform/5 mol%/24 h	>99	*Chem. Commun.*, **2016**, *52*, 8585--8588
7.	NU-GRH-1 + TMS-Cl (18 mol %)	60 °C/toluene-d_8/3 mol%/4 h	98	*ACS Catal.* **2016**, *6*, 3248−3252
8.	Uio-67-Squar/bpdc	50 °C/toluene-d_8/10 mol%/24 h	95	*J. Am. Chem. Soc.* **2015**, *137*, 919−925
9.	Cr-MIL-101-UR3	60 °C /acetonitrile/15 mol%/24 h	93	*Chem. Commun.*, **2013**, *49*, 7681--7683
10.	**CSMCRI-21**	60 °C/toluene/3.6 mol %/12 h	97	**This work**

References

1) *APEX2*, v. 2014.7-1; Bruker AXS: Madison, WI, 2014.
2) *SAINT*, v. 8.34A; Bruker AXS: Madison, WI, 2013.
3) *SADABS*, v. 2014/3; Bruker AXS: Madison, WI, 2013.
4) O. V. Dolomanov, L. J. Bourhis, R. J. Gildea, J. A. K. Howard and H. Puschmann, *J. Appl. Crystallogr.*, 2009, **42**, 339−341.
5) G. M. Sheldrick, *SHELXTL* Version 2014/7. *https://shelx.uniac.gwdg.de/SHELX/index.php.*
6) A. L. Spek, *PLATON*; The University of Utrecht: Utrecht, The Netherlands, 1999.
7) http://www.topos.ssu.samara.ru; V. A. Blatov, IUCrCompCommNewsletter 2006, 7, 4.
8) S. Nandi, D. Chakraborty and R. Vaidhyanathan, *Chem. Commun.*, 2016, **52**, 7249-7252.